Neuroscience 163 (2009) 1078–1091

NEURAL CORRELATES OF SHAPE AND SURFACE REFLECTANCE INFORMATION IN INDIVIDUAL FACES

F. JIANG,[a]* L. DRICOT,[a] V. BLANZ,[b] R. GOEBEL[c] AND B. ROSSION[a]

[a]*Unité Cognition et Développement & Laboratoire de Neurophysiologie, Université catholique de Louvain, Louvain-la-Neuve 1348, Belgium*

[b]*Fachgruppe Medieninformatik, Fachbereich 12, The University of Siegen, Siegen 57068, Germany*

[c]*Maastricht Brain Imaging Center (M-BIC), Maastricht, & F.C. Donders Centre for Cognitive Neuroimaging, Nijmegen, The Netherlands*

Abstract—Faces are recognized by means of both shape and surface reflectance information. However, it is unclear how these two types of diagnostic information are represented in the human brain. To clarify this issue, we tested 14 participants in an event-related functional magnetic resonance adaptation paradigm, with four conditions created by using a 3D morphable model: (1) repetition of the same adapting face; (2) variation in shape only; (3) variation in surface reflectance only; (4) variation in both shape and surface reflectance. Change in face shape alone was the dominant driving force of the adaptation release in functionally defined face-sensitive areas in the right hemisphere (fusiform face area [FFA], occipital face area [OFA]). In contrast, homologous areas of the left hemisphere showed comparable adaptation release to changes in face shape and surface reflectance. When both changes in shape and reflectance were combined, there was no further increased release from adaptation in face-sensitive areas. Overall, these observations indicate that the two main sources of information in individual faces, shape and reflectance, contribute to individual face sensitivity found in the cortical face network. Moreover, the sensitivity to shape cues is more dominant in the right hemisphere, possibly reflecting a privileged mode of global (holistic) face processing. **© 2009 IBRO. Published by Elsevier Ltd. All rights reserved.**

Key words: face perception, fMR adaptation, fusiform gyrus, individual faces, shape and surface reflectance.

A human face consists of two intrinsic properties: shape and surface reflectance (Bruce and Young, 1998). Surface reflectance, termed as "albedo", or "texture" in computer graphics, describes the diffuse light reflection of facial surface embedded in the three-dimensional (3D) space, and includes color. Behavioural studies have shown that in addition to face shape, surface reflectance properties are important for the perception of facial identity (e.g. Troje and Bülthoff, 1996; Lee and Perrett, 1997, 2000; Hill et al., 1997; O'Toole et al., 1999; Yip and Sinha, 2001; Vuong et al., 2005; Jiang et al., 2006; Russell et al., 2006, 2007; Russell and Sinha, 2007). For example, exaggerating the color information of a face relative to its veridical version enhances recognition performance (Lee and Perrett, 1997). Although it has been shown that face shape is the core contributor to face recognition across rotations in depth, the inclusion of the texture map also helps induce better view generalization (Hill et al., 1997), even when the main skin color is unchanged across faces (Troje and Bülthoff, 1996). Besides their diagnostic contribution, color cues could also play a supplementary rule, allowing a better segmentation of facial features, especially when shape cues are degraded (Yip and Sinha, 2001). The role of reflectance information also seemed to be more crucial in recognizing familiar faces (Russell and Sinha, 2007), supporting the hypothesis that the degree to which we rely on surface properties in general depend on our prior experience (Vuong et al., 2005).

Given that recognizing individual faces is a challenging recognition task, it is not surprising that shape and reflectance information both contribute. It has been shown that they can be about equally useful in face recognition (O'Toole et al., 1999; Jiang et al., 2006; Russell et al., 2007). Using computer graphics, O'Toole et al. (1999) manipulated shape and surface reflectance independent of each other, creating faces that varied selectively in shape or reflectance. They found roughly equal performance in an old/new recognition task for these two types of faces, showing the importance of both shape and surface reflectance for the recognition of unfamiliar faces. Similar results were reported by Russell et al. (2007) in a matching task, in which participants matched the target and distractor faces on the basis of shape or reflectance properties.

In a recent study, Jiang et al. (2006) explicitly accessed the role of shape and reflectance information in face identity adaptation, where prolonged exposure to a face alters the perception of a subsequently presented face with opposite features (Leopold et al., 2001). Significant after-effects were found after adaptation to face morphs that varied selectively in reflectance or shape. Moreover, identity after-effects induced by shape-varying or reflectance-varying faces both survived a substantial viewpoint change between the adapting and test faces. These results indicated that shape and reflectance information in faces are equally important not only for the identity adaptation but also for its transfer across changes in 3D viewpoint.

Although it is evident that both shape and reflectance information are exploited in face recognition, the exact

*Corresponding author. Tel: +32-10-47-87-41; fax: +32-10-47-37-74.
E-mail address: fang.jiang@uclouvain.be (F. Jiang).

Abbreviations: FFA, fusiform face area; fMR, functional magnetic resonance; GLM, general linear model; HRF, hemodynamic response function; IFG, inferior frontal gyrus; LO, lateral occipital; LOC, lateral occipital complex; MFG, middle frontal gyrus; OFA, occipital face area; OTS, occipitotemporal sulcus; PF, posterior fusiform; pSTS, posterior superior temporal sulcus; ROI, region of interest; SD, standard deviation; 3D, three-dimensional.

0306-4522/09 $ - see front matter © 2009 IBRO. Published by Elsevier Ltd. All rights reserved.
doi:10.1016/j.neuroscience.2009.07.062

nature of their neural representations remains largely unclear. The results from Jiang and her colleagues (2006) suggested that the representations of both shape and surface reflectance information in faces are retained up to a level that supports view generalization. Thus, surface reflectance information, as well as shape information, may be part of high-level face representations. At an early neural level, it is known that shape and surface reflectance information are processed in partially segregated visual areas and pathways (e.g., Tovee, 1996; Grill-Spector and Malach, 2004). Given that these two kinds of information appear integrated when we perceive individual faces, and the inclusion of both these kinds often result in superior behavioural performance, we might speculate that the integration could take place in high-level visual areas. It has not been examined, however, at the level of the high-level visual areas, whether shape and surface information retain unique representations, or integrate into a single representation.

The purpose of the present study was to address this issue by means of neuroimaging. Precisely, we aimed to first identify areas that represent shape and surface reflectance information diagnostic for individual faces in the human brain. Based on previous neuroimaging studies, several brain areas within the human occipitotemporal cortex that show greater sensitivity to faces than other object categories (Haxby et al., 2000; Sergent et al., 1992) were our candidates. These areas have been defined in the middle fusiform gyrus ("fusiform face area" or "FFA", Kanwisher et al., 1997), the inferior occipital cortex ("occipital face area" or "OFA", Gauthier et al., 2000), and the posterior part of the superior temporal sulcus (pSTS, e.g. Puce et al., 1998). These three areas are assumed to form the core network for face perception in the human brain (Haxby et al., 2000; Ishai, 2008). They are bilateral, but with a strong right hemispheric dominance that has been associated with the perception of the face stimulus as a global configuration (Rossion et al., 2000; Schiltz and Rossion, 2006; Harris and Aguirre, 2008). The exact interconnections between these face areas are largely unknown, although they are thought to be essential for normal face perception (Rossion et al., 2003; Fox et al., 2008a; Thomas et al., 2008). Second, we wanted to examine the nature of the representation of face shape versus reflectance information in these areas. Specifically, we wanted to know whether the representations of shape and reflectance information in faces remain separated or become integrated in high-level visual areas that are sensitive to individual faces.

To achieve these goals, we used a functional magnetic resonance adaptation paradigm (fMR adaptation, Grill-Spector et al., 1999; Grill-Spector and Malach, 2001; for a review see Grill-Spector et al., 2006). fMR adaptation refers to the suppression of activation induced by the repeated representation of an identical stimulus. By manipulating certain attributes of the second stimulus with respect to the adapting stimulus, fMR adaptation can be used to study the selectivity and invariance property of targeted neural populations (Grill-Spector et al., 2006). For example, the FFA and OFA both show a larger neural response (release from adaptation) when two different individual faces are presented as compared to a repeated presentation of the same face (Gauthier et al., 2000; Grill-Spector and Malach, 2001; Schiltz and Rossion, 2006; Gilaie-Dotan and Malach, 2007). This indicates that these areas are sensitive to the identity of the face, while the same method has shown that the pSTS is more sensitive to facial expression (Winston et al., 2004).

In our fMR adaptation paradigm, we selectively varied the shape or reflectance property of the test face with respect to the adapting face. Four experimental conditions were included: (1) repetition of the exact same face stimulus (same); (2) variation in shape only (shape-different); (3) variation in surface reflectance only (reflectance-different); (4) variation in both shape and surface reflectance (both-different). Note that such selective manipulation of different properties of objects has been implemented successfully in recent studies (e.g., Kourtzi and Kanwisher, 2000, 2001; Kourtzi et al., 2003).

The amount of release from fMR adaptation in the shape-different, reflectance-different, and both-different conditions was then taken as an indicator to examine the nature of shape versus reflectance codes. We consider several possible outcomes. If the representation of shape and reflectance was segregated in the cortical face network, we would find face-sensitive areas that selectively release from adaptation from changes in shape but not reflectance property, or vice versa. Alternatively, if the two sources of information were integrated in face-sensitive brain areas, sensitivity to shape and reflectance changes would be observed in the same face-sensitive area(s). Furthermore, if the integration of face shape and reflectance in the coincident face-sensitive area(s) was additive in nature, we would observe enhanced adaptation release in the both-different condition, in which both shape and reflectance cues were present simultaneously. This additive integration could account for behavioral facilitation induced by the inclusion of both shape and reflectance information.

EXPERIMENTAL PROCEDURES

Participants

Fourteen participants (11 females and three males; mean age 24) were included in the study. All participants were right-handed and had normal or corrected vision. Written informed consent was obtained from all participants prior to the experiment, following procedures approved by University of Maastricht where all imaging took place.

Stimuli

Stimuli used in this experiment were generated with a 3D morphable model (Blanz and Vetter, 1999) that implemented a multidimensional face space based on 200 3D face scans. This model transforms the 3D shape (x, y, z) and surface reflectance (r, g, b) of a face into separate vectors constructed from 75,000 surface points in correspondence with a reference face. With corresponding points determined by an optical flow algorithm described in Blanz and Vetter (1999), the reflectance of one face can be

mapped on to the shape of another face, resulting in a realistically looking new face with both physical and perceptual differences.

Using this model, we created shape-different and reflectance-different faces by exchanging the shape and reflectance properties between a pair of faces. Specifically, we picked 40 original faces (half female) from the face space and split them into 20 gender-matched pairs. Each pair consisted of two original faces, for example, A and B. From these two original faces, we created two additional faces—AB and BA. We used two letters to describe faces created from their original parents, with the first letter indicating the origin of their shape and the second indicating the origin of their reflectance. Face AB was created by mapping the reflectance of face B onto the shape of A, and face BA was created by mapping the reflectance of face A onto the shape of B. Therefore, face AB differed from face A in reflectance and from face B in shape, while face BA differed from face A in shape and from face B in reflectance. Also note that face AB and BA were different in both shape and surface reflectance map. An example pair of original faces and their AB and BA version are shown in Fig. 1A.

To quantify the physical difference induced by changes in shape, reflectance, and both, we calculated intensity-based (range 0–255) Euclidean distance per pixel between adapting and test stimuli. The averaged distance (mean±standard deviation (SD)) between image pairs was 35.71±6.26 in the shape-different condition, and 22.89±5.05 in the reflectance-different condition. Note that these differences are thought to reflect natural variations in shape and reflectance properties of the faces as captured by 3D face scanner, and were not equalized artificially for the purpose of the experiment (i.e. testing how face-sensitive areas code for natural variations in shape and reflectance cues). When the two cues were combined (both-different condition), the averaged distance was 45.63±7.27.

Design and procedure

The experiment consisted of an event-related adaptation paradigm. Participants were asked to match the identity of paired adapting and test faces and judge whether the test face was the same as the adapting face or different. The shape and surface reflectance properties of the test face were manipulated with respect to the adapting face. As shown in Fig. 1B, four test conditions were included: (1) repetition of the same adapting face (same); (2) variation in shape only (shape-different); (3) variation in surface reflectance only (reflectance-different); (4) variation in both shape and surface reflectance (both-different). Participants were informed that the difference between two faces, if there was any, could be either in the shape, in the reflectance, or in both. A "different" response was required for the shape-different, reflectance-different, and both-different conditions.

Each participant performed four experiment runs. Each run lasted approximately 16 min. For each run, we presented a total of 80 trials (20 for each experimental condition) with faces generated from five pairs of original faces. Trials were presented randomly for each run and for each participant. Note that each face was used equally as an adaptor or as a test stimulus both within and across experimental conditions (see Table 1 for 16 trials formed from a pair of original faces).

In each trial, an adapting face was presented for 500 ms, followed by a blank screen for 500 ms. A test face was then presented for 500 ms, followed by two blank screen (750 ms each)

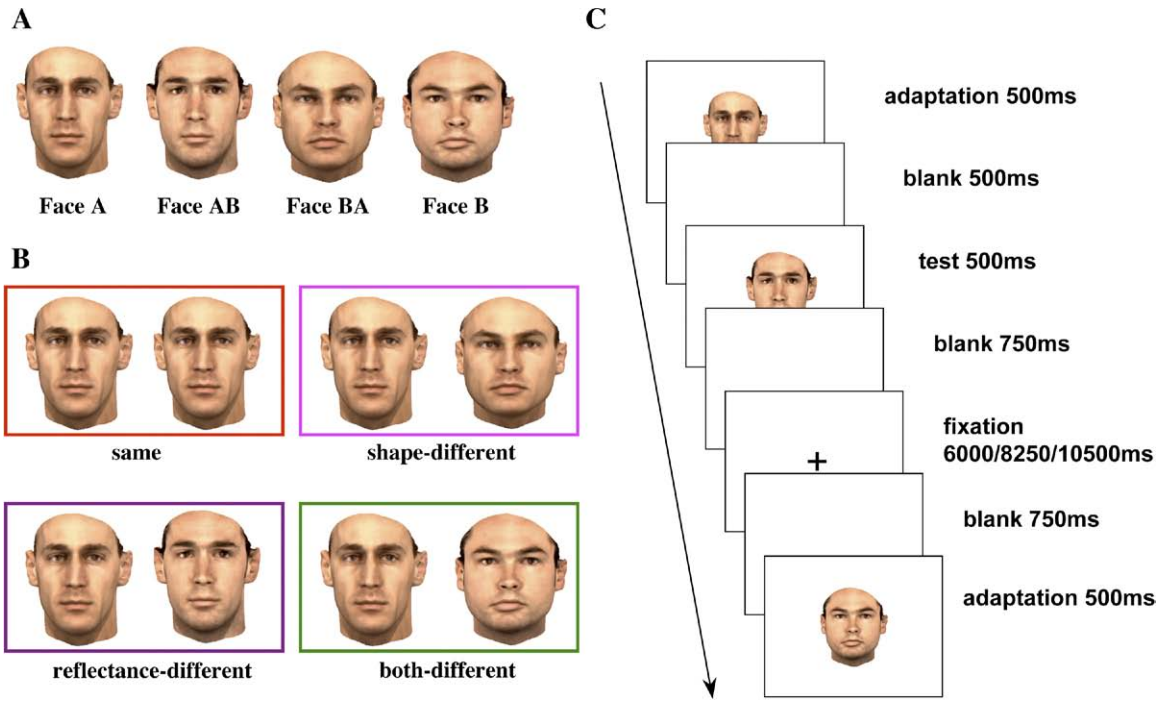

Fig. 1. Example stimuli and trail. (A) Illustration of an example pair of original faces (A and B) and corresponding faces (AB and BA) created with a 3D morphable model (Blanz and Vetter, 1999) by exchanging the shape/surface reflectance between two original faces. Face AB was created by mapping the reflectance of face B onto face A's shape, while face BA was created by mapping the reflectance of face A onto face B's shape. (B) Illustration of experimental conditions. Conditions were defined by the shape and surface reflectance properties of the test stimulus with respect to the adapting stimulus. Four conditions were included: repetition of the same adapting face (Same); variation in shape only (Shape-different); variation in surface reflectance only (Reflectance-different); and variation in both shape and surface reflectance (Both-different). (C) Illustration of experiment trial. Both adapting and test face were presented for 500 ms and were separated by a 500 ms blank screen. A long fixation with duration varying randomly trial by trial (6000/8250/10,500 ms) was presented to ensure that the onsets of two subsequent trials were separated by at least 9000 ms. For interpretation of the references to color in this figure legend, the reader is referred to the Web version of this article.

Table 1. Illustration of 16 trials (four trials per condition) generated from one pair of original faces (A and B) and their shape/reflectance-different versions (AB and BA)

Condition	Adapting face	Test face
Same	A	A
	B	B
	AB	AB
	BA	BA
Shape-different	A	BA
	B	AB
	AB	B
	BA	A
Reflectance-different	A	AB
	B	BA
	AB	A
	BA	B
Both-different	A	B
	B	A
	AB	BA
	BA	AB

Each face was used equally as an adaptor or as a test face both within and across conditions.

For face AB and BA, the first letter refers to the origin of face shape, and the second letter refers to the origin of face reflectance.

and a fixation cross with duration varying randomly among 6000, 8250, and 10,500 ms (Fig. 1C). This timing ensured that the onsets of any two subsequent trials were separated by 9000–13,500 ms (4–6 TRs), for the purpose of reducing overlapping hemodynamic responses.

Stimuli were back projected onto a screen located over participants' heads. PC running E-prime 1.1 (PST Inc., Pittsburgh, PA, USA) was used to present stimuli and collect behavioral responses. All the stimuli were presented in color. The adapting face was always presented in the center of the screen, while the location of the test face was jittered randomly trial by trial with respect to the adapting stimulus. The range of shift in both X and Y axe was within ±50 pixels (±0.908 cm/±0.9125° visual angle). The test face was also 10% larger than the adapting face. We used location shift and size change to avoid pixel-wise matching and to minimize low-level stimulus repetition confounds.

Localizer scans

Independent localizer scans were performed to localize areas responding preferentially to faces and to verify the response properties of regions derived from whole brain analysis. Each participant conducted two runs, in which they viewed blocks of faces, cars, phase-scrambled faces, and phase-scrambled cars, and performed a one-back matching task. Each run lasted 11 min and consisted of 24 alternating blocks (18 s each) with 9 s fixation in between. During each block, 18 images were presented for 750 ms followed by a 250 ms blank screen. All images of faces and cars were presented in color with equalized luminance and their scrambled version was created with Fourier phase randomization (e.g., Sadr and Sinha, 2004).

Image acquisition

All the participants were scanned at the Maastricht Brain Imaging Center. Data were collected using a 3T head scanner (Siemens, Allegra, Germany). Functional data were obtained from 36 transverse slices with a spatial resolution of 3.5×3.5×3.5 mm^3 (acquisition matrix, 64×64), using a repeated single-shot echo-planar imaging sequence (TE=50 ms, TR=2250 ms, FA=90°, FOV=224 mm). High-resolution structural images were obtained with 1×1×1 mm^3 spatial resolution (acquisition matrix, 256×256), using ADNI sequence (TE=2.6 ms, TR=2250 ms, FA=9°, FOV=256 mm). These T1-weighted images provided detailed anatomical information. A 25° angle perpendicular to the main magnetic field B_0 was used to reduce magnetic artifacts and signal dropout, allowing us to record up to the anterior inferior temporal lobe (Deichmann et al., 2003).

Behavioral data analysis

Participants' behavioral responses were collected during fMRI experiment. Accuracy in identity matching and mean correct response time were computed for each of the four conditions (Fig. 2) and were tested with one factor repeated analysis of variance (ANOVA). Post hoc test (Scheffé test) was then used to compare between conditions.

fMRI data analysis

Data were analyzed using Brain Voyager QX (Version 1.10, Brain Innovation, Masstricht, the Netherlands). The first four volumes of each functional dataset were discarded to cope with T2* contrast saturation effect. Prior to statistical analysis, the functional data underwent a series of preprocessing steps, namely slice scan time correction, 3D motion correction (with realignment to the first volume), linear trend removal, and high pass filtering (removing frequencies lower than 3 cycles/session, ≈0.003 Hz for experimental runs and 0.005 Hz for localizer runs). No spatial smoothing was applied to the functional data. Both anatomical and functional data were transformed into Talairach space (Talairach-transformation; Talairach and Tournoux, 1988). The statistical analysis was based on a general linear model (GLM), in which predictor time course was obtained by convolution of a stick function with a two-gamma hemodynamic response function.

The areas responding preferentially to faces were defined independently for each individual participant from localizer scans, using the contrast (faces–cars) in conjunction with the contrast (faces-scrambled faces). This conjunction analysis ensured that the activation in face-sensitive regions was not related to low-level

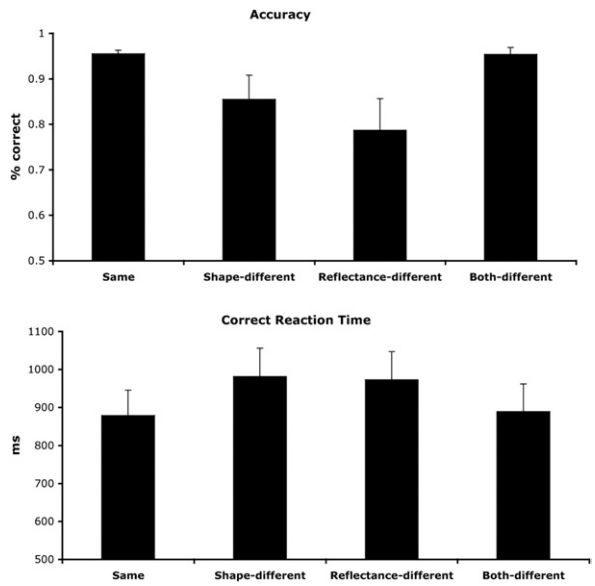

Fig. 2. Behavioral results. Response time was calculated based on correct trials only.

differences between faces and non-face object categories, as could be the case in a classical fMRI face localizer (faces-objects). Before identifying regions individually, we first performed a GLM on localizer scans from all participants. Clusters that show a significant effect (P(Bonf)<0.05) were identified and were used as a guideline for the selection of individual regions of interest (ROIs). Among these clusters, we only selected the ones that we could consistently identify in most of the participants as our ROIs. Based on this criterion, we included bilateral FFA and OFA for further analysis. We also included the right pSTS for completeness, although we only could identify it in half of the participants.

For each participant, all contiguous voxels in the middle fusiform gyrus and inferior/middle occipital gyrus, significant at q(false discovery rate, FDR)<0.001 were selected (FFA and OFA, respectively). We raised statistical threshold for two participants to separate their overlapping fusiform and inferior occipital activation. We also lowered the q(FDR) to 0.05 for three participants to localize OFA, due to relatively smaller size of their regions.

To test our hypothesis, we investigated fMR adaptation effects in individually defined ROIs. The analysis was time locked to the onset of the test face (i.e., the second face) in each trial. Specifically, for each subject and each ROI, the beta weights associated with experimental conditions (i.e., the coefficients of predictor time course) were estimated. To examine the release from adaptation and to compare the magnitude of adaptation release, these beta weights were then tested with pre-defined contrasts for a random effect at the group level. Note that due to the lack of statistical power, we performed an ROI based fixed-effect GLM analysis for the right pSTS.

Using the "same" condition as a baseline, we calculated the difference in beta weights to reveal the magnitude of release from adaptation induced by different face cues (i.e., face shape, face reflectance, or both) in each ROI (Fig. 3). To show that the effects we reported here reflect the true hemodynamic response function (HRF), we computed the condition related average time courses in each ROI (Fig. 4). Specifically, in each ROI, a mean time course was extracted across all the voxels for each of the four experimental conditions and the extraction was done for each participant separately. These time courses were then averaged across participants for each condition in each ROI. Note that we present the time course plots for illustration purposes only, not for statistical inference. The GLM analysis in Brain Voyager takes into account all time points of the HRF, and thus, is more sensitive and powerful than a peak analysis.

We also performed a whole brain analysis to highlight brain regions that are sensitive to change in face shape, reflectance, or both, without prior external localization. A multi-subject random-effects GLM was carried out independently for each voxel. Brain regions sensitive to shape or/and reflectance information were then identified by corresponding contrast. Clusters that showed a significant effect ($P<0.01$ uncorrected, one-tailed t-test, post corrected by cluster size thresholding of 7 (i.e., 189 mm^3)) were recognized and reported (Figs. 5 and 6). We increased threshold for contrast (shape-different–same) to separate overlapping fusiform and occipital activation (Table 2). We further examined the face preference of identified clusters using contrasts (faces–cars) and (faces–scrambled faces) on the time course data extracted from localizer scans. A cluster was recognized as face-preference only when both contrasts were significant.

Post-scanning behavioral test with new participants

To test whether the magnitude of fMR adaptation release we found reflected the perceptual dissimilarity of faces, we carried out an additional behavioral test with nine new participants (five females; mean age, 24) on a PC laptop. The design was identical to that used in the scanner, except that instead of matching pair of faces, participants judged the similarity between the adapting and test faces on a scale of 1 (very dissimilar) to 7 (very similar). The similarity rating for each pair of adapting and test faces was then converted to dissimilarity measure (i.e., distance) using 7-rating. The perceptual distances for the four conditions were tested with one factor repeated measures ANOVA and post hoc Scheffé test.

Finally, to understand better the pattern of adaptation release we found, we also tested twelve participants (eight females; age 24 ± 3) behaviorally to examine the relative dependence of shape and surface reflectance information on a central aspect of individual face processing, i.e. configural/holistic processing. Specifically, we examined how discrimination performance on the basis of shape or/and reflectance information was affected by picture–plane inversion, a manipulation that is known to disrupt holistic face processing (Farah et al., 1995; Rossion, 2008). Participants performed a delayed match-to-sample, two-alternative forced-choice task that was similar to that used in Russell et al. (2007). An example of inverted trial was shown in Fig. 7A. The matching task could be performed based on face shape, surface reflectance, or both. Upright and inverted trials were grouped in different blocks, whose order was counterbalanced between participants. The decrease of accuracy caused by inversion was further tested with planned t-tests.

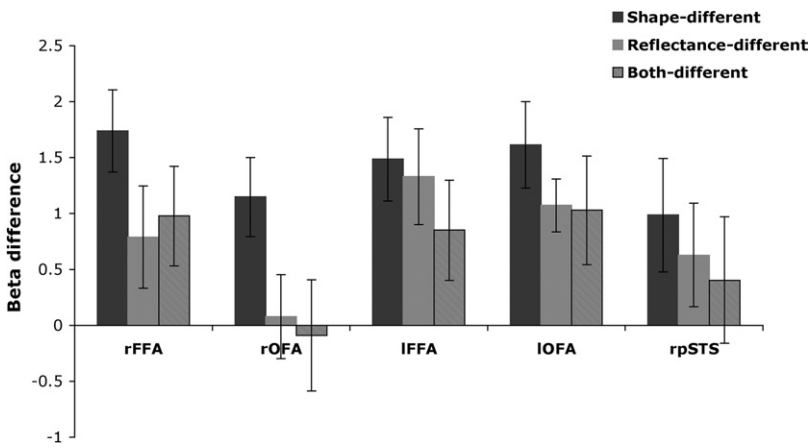

Fig. 3. Illustration of the magnitude of release from adaptation in face-sensitive ROIs induced by changes in face shape alone (shape-different, black bars), face reflectance alone (reflectance-different, grey bars), or both (both-different, diagonal bars). Beta weights difference was calculated using beta weights in the same condition as baseline.

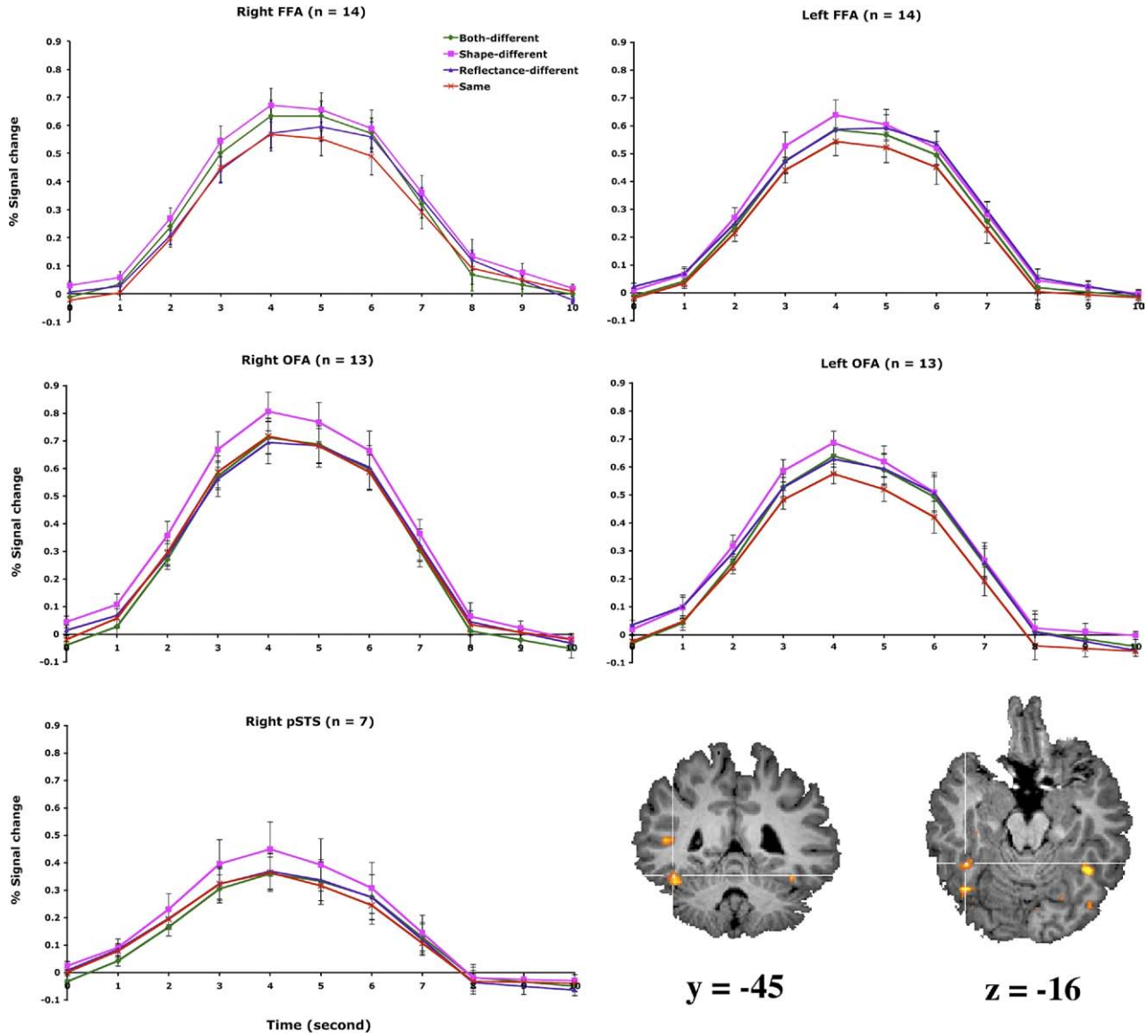

Fig. 4. Averaged time course of the neuronal responses in face-sensitive ROIs measured in event-related adaptation experiment. The average percent signal change (±SE, $n=14$ of FFA, $n=13$ for OFA, and $n=7$ for rpSTS) is plotted for the four experimental conditions, in which participants viewed the same adapting face (same), a face varied in shape (shape-different), a face varied in reflectance (reflectance-different), or a face varied in both shape and reflectance (both-different), following adaptation. With cross on the right FFA, a transverse slide ($z=-16$) and a coronal slide ($y=-45$) through the brain of a participant illustrate the ROIs responding preferentially to faces as localized by contrast (faces–cars) in conjunction with contrast (faces–scrambled faces) in external localizer scans. For interpretation of the references to color in this figure legend, the reader is referred to the Web version of this article.

RESULTS

In-scanner behavioral results

Participants performed well in the identity matching task during the fMRI experiment, with an overall average accuracy of 89%. The matching accuracy in the four experiment conditions differed significantly ($F(3,39)=5.32$, $P<0.004$). As seen in Fig. 2, participants were less accurate in the shape-different and reflectance-different conditions than in the same and both-different conditions ($F(1,39)=14.11$, $P(F_{\text{scheffé}})<0.007$). A significant difference was also found for correct response time ($F(3,39)=4.89$, $P<0.006$), with longer response time in the reflectance-different and shape-different conditions than in the same and both-different conditions ($F(1,39)=14.48$, $P(F_{\text{scheffé}})<0.006$), indicating no evidence of speed-accuracy trade-offs. There was no difference in both accuracy ($F(1,39)=1.83$, ns) and response time ($F(1,39)=0.1$, ns) between the shape-different and reflectance-different conditions. These results suggest that whereas either shape or surface reflectance alone is important for differentiating individual faces, the integration of the two gives rise to superior performance.

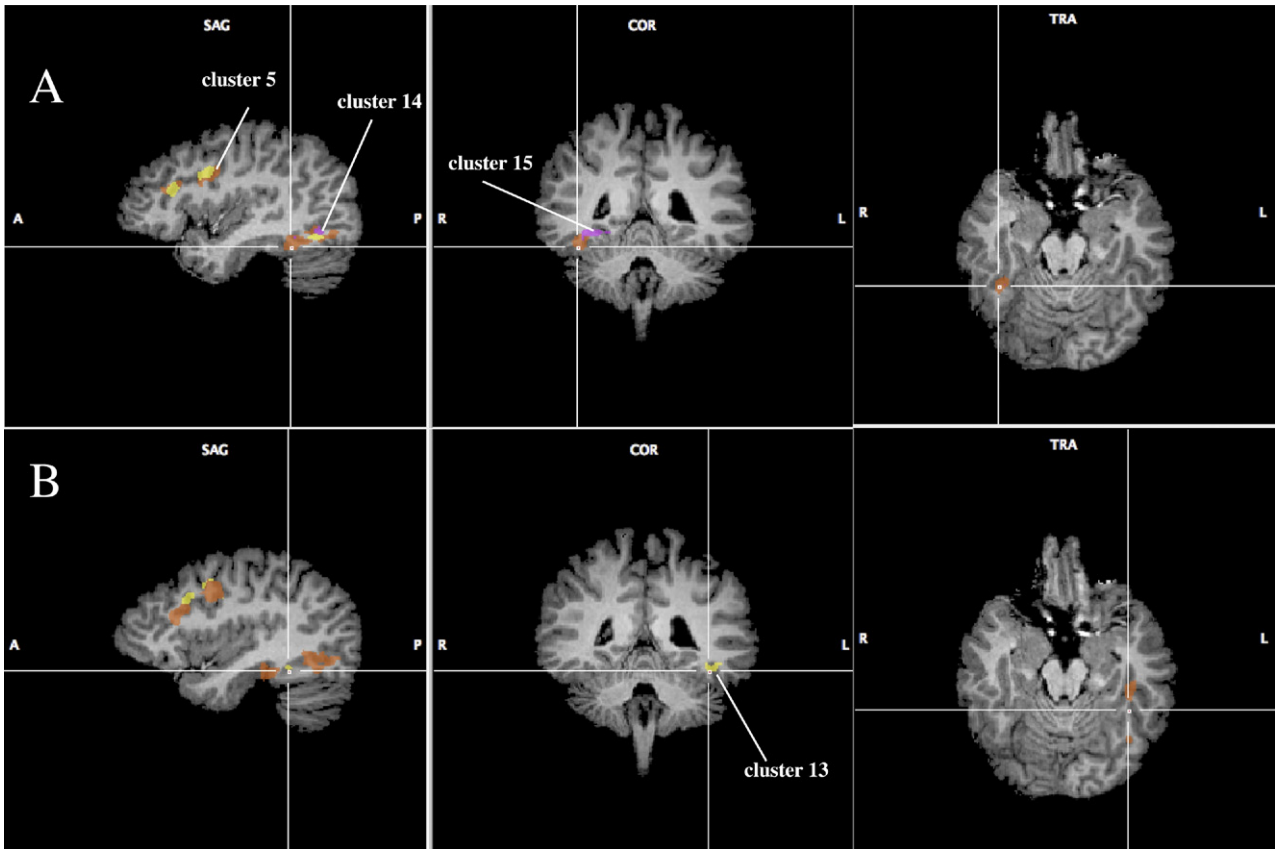

Fig. 5. Whole-brain GLM maps displaying clusters reported in Table 2. Cluster revealed by contrast (shape-different–same), (reflectance-different–same), and (both-different–same) are colored in orange, yellow, and purple, respectively. The top row is positioned at the average coordinates of the right FFA (39, −44, −17) and the bottom row is positioned at the average coordinates of the left FFA (−38, −43, −16). We further indicated clusters whose time course data were reported in Fig. 6. All three maps shown here were initially thresholded at $P<0.01$ (one tailed, $t(13)=2.65$), post corrected by cluster size thresholding of 7 (189 mm^3). Note that clusters 1–4 reported in Table 2 for contrast (shape-different–same) were obtained with higher statistical threshold in order to separate overlapping fusiform and inferior occipital activation. For interpretation of the references to color in this figure legend, the reader is referred to the Web version of this article.

Post-scanning behavioral test results

The perceptual distance between the adapting and the test faces differed significantly across experimental conditions ($F(3,24)=202.93$, $P<0.0001$). Participants rated pairs from the both-different condition as most dissimilar (mean perceptual distance 4.49 ± 0.60, $F(1,24)=305.14$, $P(F_{scheffé})<0.00001$) and pairs from the same condition as most similar (mean perceptual distance 0.125 ± 0.1, $F(1,24)=392.95$, $P(F_{scheffé})<0.00001$). Moreover, pairs of adapting and test faces from the "shape-different" condition were perceived more dissimilar than pairs from the "reflectance-different" condition (mean perceptual distance 3.28 ± 0.63 and 2.15 ± 0.31 respectively, $F(1,24)=38.20$, $P(F_{scheffé})<0.0001$). These results indicate that the overall perceptual difference between faces was determined by both shape and reflectance information in the faces, albeit with a stronger reliance on face shape.

In the delayed matching task, participants performed less accurately and responded more slowly for inverted than in upright faces (Fig. 7B), as revealed by a main effect of inversion ($F(1,11)=29.99$, $P<0.001$ and $F(1,11)=5.39$, $P<0.05$, respectively). There was a main effect of condition for both accuracy and correct response time ($F(2,22)=52.28$, $P<0.001$ and $F(2,22)=17.92$, $P<0.001$, respectively), with better and faster performance when the shape and reflectance cues were combined (i.e., both-different condition, Fig. 7B). Most importantly, there was a significant interaction between inversion and condition for accuracy ($F(2,22)=4.45$, $P<0.03$). As predicted, planned t-tests showed a significant larger accuracy decrease with inversion in the shape-different condition than the reflectance-different condition ($P<0.02$, one tailed) and than the both-different condition ($P<0.01$, one tailed), with no significant difference between these latter two conditions ($P>0.47$, ns). These results indicate that the processing of shape information was disrupted to a greater extent than that of reflectance information or the combination of shape and reflectance information.

Face-sensitive ROI results

Before identifying regions individually, we performed a GLM analysis on localizer scans from all the participants. This multi-subject GLM identified brain areas activated more to faces than to objects and scrambled faces, includ-

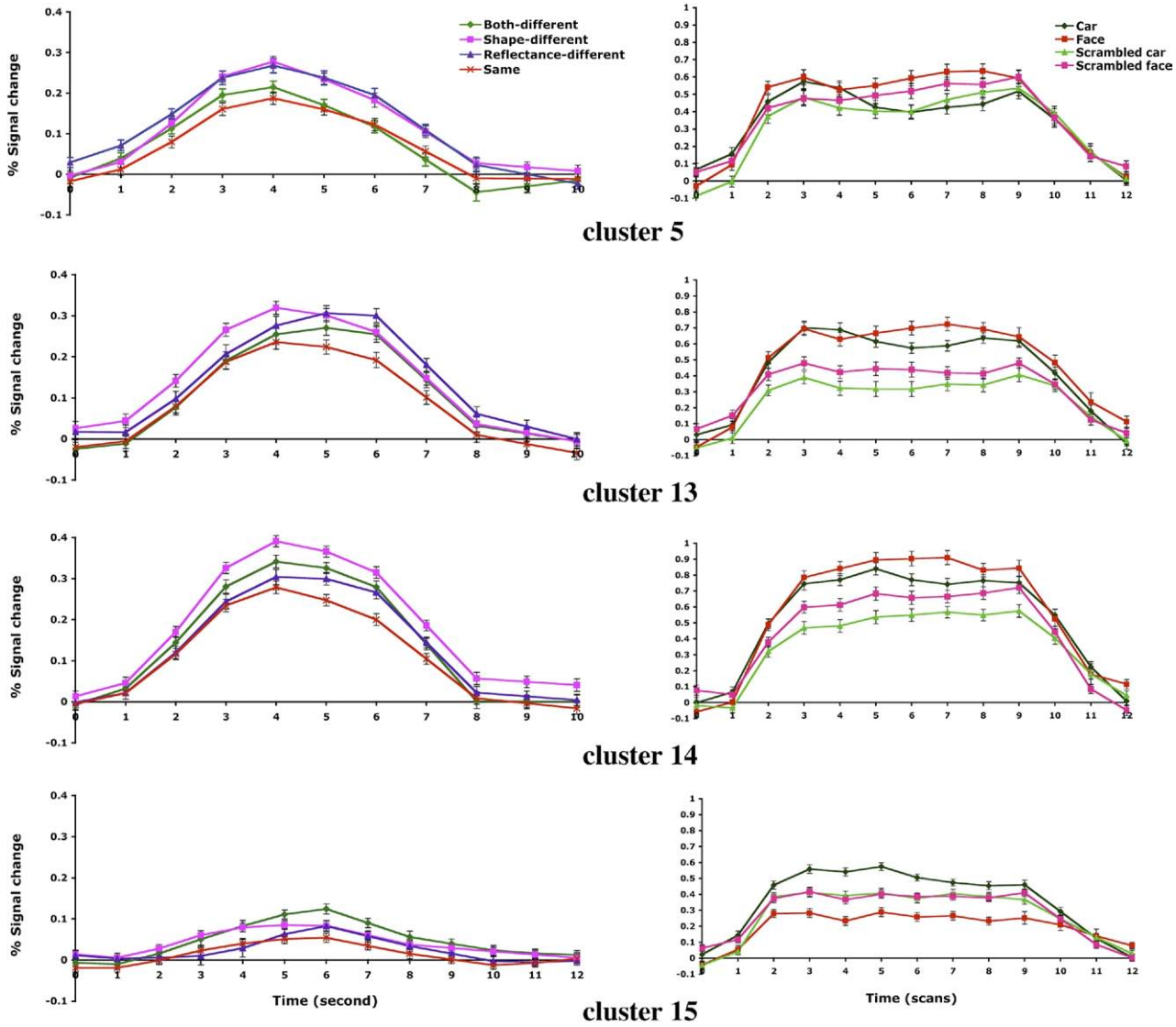

Fig. 6. Time course data extracted from representative clusters revealed by whole brain analysis. For each cluster, condition related percent signal change was averaged across runs for each subject and then across subjects. Both experimental (left column) and localizer data (right column) are shown for cluster 5 (right IFG), cluster 13 (left fusiform gyrus), cluster 14 (right occipital gyrus), and cluster 15 (right PF/OTS). For interpretation of the references to color in this figure legend, the reader is referred to the Web version of this article.

ing bilateral FFA, OFA, pSTS, bilateral amygdala, the right anterior IT, and the right inferior frontal gyrus (IFG). This coarse analysis gave us an overview of the face network, and also a guideline for the selection of ROIs on an individual basis. We focused our further analysis on bilateral FFA and OFA, which we could successfully identify in most of our participant (see Localizer scans session).

Right FFA. Significant release from adaptation was found in the right FFA as a consequence of changes that mainly involved face shape, with or without the presence of changes in face reflectance. As seen in Fig. 3, compared to the same condition, there was a significant larger response in the right FFA (Talairach coordinates, mean±SD, voxel size±SD, 39±4, −44±7, −17±4, 519 voxels±282, n=14/14), in the shape-different and the both-different conditions ($t(13)=4.733$, $P<0.0004$ and $t(13)=2.203$, $P<0.05$, respectively). Although there was a delayed increase in activation for reflectance-different faces (Fig. 4), this difference did not reach significance ($t(13)=1.735$, ns). The magnitude of adaptation release induced by face shape alone was significantly larger then that induced by face reflectance alone ($t(13)=3.113$, $P<0.01$), but was not different then that induced by the combination of face shape and reflectance ($t(13)=1.523$, ns).

Left FFA. Changes in either face shape or face reflectance alone evoked significant adaptation release in the left FFA (−38±4, −43±8, −16±3, 477 voxels±462, n=14/14). Stronger adaptation effects were observed in both shape-different ($t(13)=3.961$, $P<0.002$) and reflectance-different condition ($t(13)=3.095$, $P<0.009$). The

Table 2. Significant clusters revealed by whole brain random-effect GLM analysis

Cluster	Talairach coordinates			Size (mm^3)	$t(13)$	P*	Face-pre**	Location
	x	y	z					
Contrast: shape-different–same								
1	38	−45	−13	713	4.5	$P<0.0003$	Yes	Right fusiform gyrus
2	42	−60	−8	933	4.5	$P<0.0003$	Yes	Right occipital gyrus
3	−40	−30	−15	593	3.13	$P<0.004$	Yes	Left anterior fusiform gyrus (lateral occipitotemporal sulcus)
4	−40	−58	−9	1526	3.13	$P<0.004$	No	Left occipital gyrus (posterior part of fusiform gyrus)
5	42	7	28	955	2.65	$P<0.01$	Yes	Right IFG
6	45	31	18	1331	2.65	$P<0.01$	Yes	Right MFG
7	−38	5	33	1641	2.65	$P<0.01$	Yes	Left IFG
8	−43	23	19	2212	2.65	$P<0.01$	No	Left MFG
Contrast: reflectance-different–same								
9	44	10	28	1118	2.65	$P<0.01$	Yes	Right IFG
10	43	29	18	550	2.65	$P<0.01$	Yes	Right MFG
11	−39	7	32	1145	2.65	$P<0.01$	Yes	Left IFG/MFG
12	39	−59	−9	235	2.65	$P<0.01$	Yes	Right occipital gyrus
13	−42	−45	−12	284	2.65	$P<0.01$	Yes	Left fusiform gyrus
Contrast: different–same								
14	41	−59	−6	355	2.65	$P<0.01$	Yes	Right occipital gyrus
15	32	−41	−9	685	2.65	$P<0.01$	No	Right posterior fusiform gyrus (lateral occipitotemporal sulcus)

* Uncorrected P values (one tailed), post corrected by cluster size thresholding of 7 (189 mm^3).
** Face-preference was measured with contrast (faces–cars) and (faces–scrambled faces).

amount of adaptation release in these two conditions did not differ ($t(13)=0.542$, ns). A trend was also observed for the both-different condition, when its activation was contrasted with the repetition of the same faces ($t(13)=1.908$, $P<0.08$).

Right OFA. In the right OFA (38±6, −67±10, −11±4, 264 voxels±201, $n=13/14$), only changes in face shape induced a higher response ($t(12)=3.26$, $P<0.007$). No significant adaptation release was observed in the reflectance-different ($t(12)=0.213$, ns) condition. There was no significant adaptation release for the both-different condition in the right OFA ($t(12)=-0.178$, ns). We suspected that this failure was mainly due to the fact that the right OFA was defined relatively posterior for some of the participants. This was confirmed by the whole brain analysis, in which a more anterior cluster in the right occipital lobe (center 41, −59, −6, see cluster 14 in the Whole brain analysis section below) showed significant adaptation release in the both-different condition.

Left OFA. Similar to the left FFA, the left OFA was also equally sensitive to changes in face shape and face reflectance. Specifically, in the left OFA (−35±7, −68±9, −12±4, 201 voxels±275, $n=13/14$), a higher response than the same condition occurred when participants viewed both shape-different faces ($t(12)=4.161$, $P<0.001$) and reflectance-different faces ($t(12)=4.529$, $P<0.0007$). The adaptation induced by face shape alone was not significantly different than that induced by face reflectance alone ($t(12)=1.6$, ns). There was also a trend of release from adaptation in the both-different condition ($t(12)=2.121$, $P<0.06$).

Right pSTS. The right pSTS was identified reliably on seven participants (49±6, −38±9, 8±6403 voxels±329, $n=7/14$). Significant adaptation release occurred only in shape-different condition ($t=2.64$, $P<0.008$). We believe that the data from the right pSTS could be informative; however, we hesitate to directly compare them to those from regions of the ventral stream and draw any firm conclusions. Face localizers using dynamic stimuli (e.g., Fox et al., 2008b) may help in the future to further examine the differences in shape and reflectance processing between regions of the dorsal and ventral streams.

In the face sensitive regions we defined, as seen in Fig. 3, it is clear that shape information, when presented alone, showed strong modulation on adaptation release. This was especially evident in the right hemisphere, where changes in face shape produced significantly larger adaptation release than changes in face reflectance did. On the other hand, regions identified in the left hemisphere showed roughly equal sensitivity to face shape and reflectance. However, the combination of face shape and face reflectance cues, as presented simultaneously in the both-different condition, did not elicit higher adaptation release than that elicited by any one of the cues alone in the face sensitive regions defined in the current study.

To test the hemispherical difference in shape and reflectance processing, we calculated a shape/reflectance ratio using ($beta_{shape\text{-}different}/beta_{reflectance\text{-}different}$) for bilateral FFA and OFA. Given the fact that the beta weights in both shape-different and reflectance-different conditions were positive, a shape/reflectance ratio greater than 1 reflects a stronger sensitivity to face shape than to face

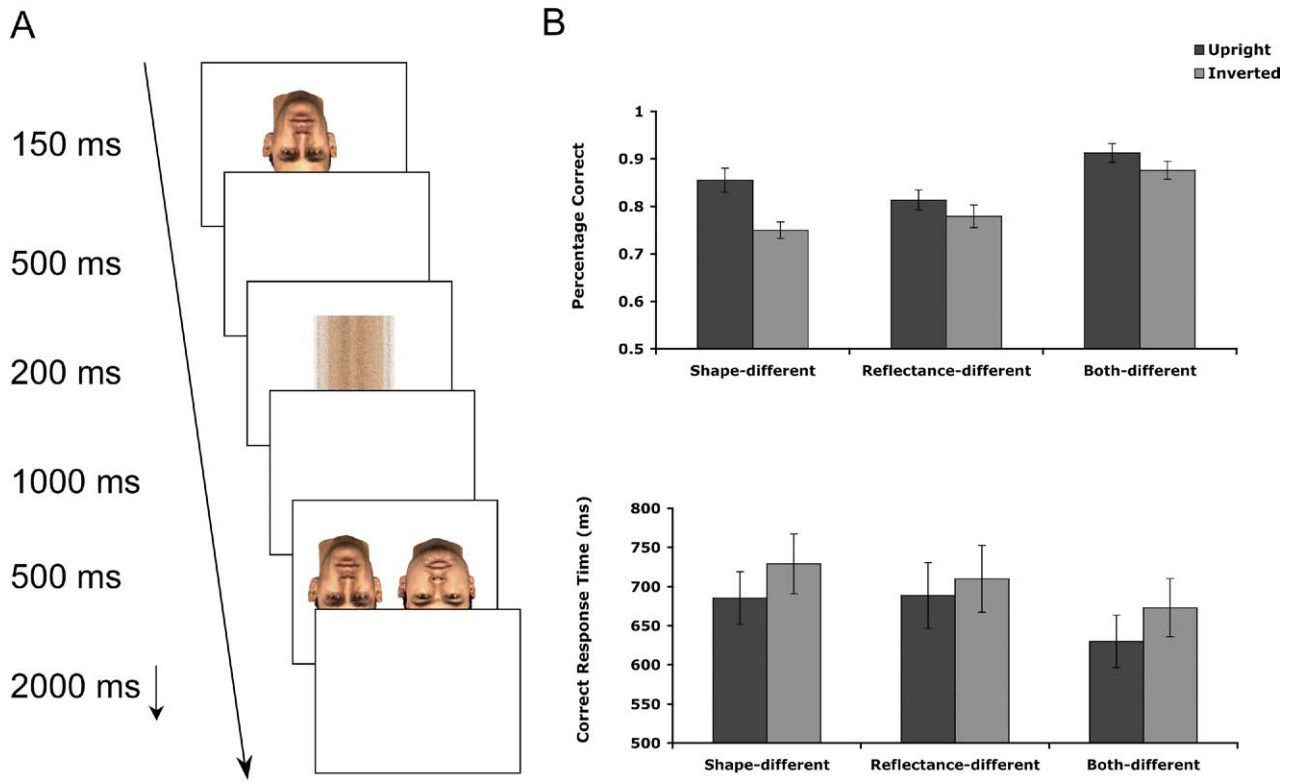

Fig. 7. Post-scanning delayed matching task. (A) An example of inverted trial. (B) Results including percentage correct and correct response time. For interpretation of the references to color in this figure legend, the reader is referred to the Web version of this article.

reflectance. For FFA, this ratio was significantly larger in the right hemisphere (mean±SD, 1.10±0.13) than in the left hemisphere (1.02±0.1, $F(1,13)=8.79$, $P<0.011$). Although there was also a trend for OFA, the effect of hemisphere did not reach significance ($F(1,12)=2.96$, $P=0.11$).

Whole brain analysis

Without prior localization, a whole brain random-effect GLM analysis was performed to identify brain regions sensitive to changes in face shape, face reflectance, and both. Clusters reported here were based on an uncorrected *P* value of 0.01 (one-tailed) in combination with cluster size thresholding (Table 2, Fig. 5). The results from the whole brain analysis are largely consistent with our ROI based results. Here, we only point out several complementary findings.

First, clusters in bilateral dorsolateral prefrontal cortex were found to release from adaptation for changes in either shape or reflectance alone (Fig. 5 sagittal view). As indicated by their activation profiles (see Fig. 6 for time course data extracted from right IFG, cluster 5 in Table 2), these regions showed relatively higher activation for shape-different and reflectance-different conditions than for the different and same conditions. This unique activation pattern suggests that the dorsolateral prefrontal activation might reflect task difficulty (Philiastides and Sajda, 2007), given that participants were less accurate and slower in shape-different and reflectance-different conditions.

Second, three overlapping clusters were found in the right occipital gyrus (Fig. 5A sagittal view), including cluster 2 defined by the contrast (shape-different–same), cluster 12 defined by the contrast (reflectance-different–same), and cluster 14 defined by the contrast (both-different–same). Note that although these face-sensitive clusters are in the right occipital gyrus, they are more anterior than individually defined OFA. These three clusters showed similar activation profile, with large adaptation release in the shape-different condition (see time course data from cluster 14, Fig. 6). These overlapping clusters showed sensitivity to changes in face shape and reflectance, separately or combined, however, they did not show stronger adaptation release in the both-different condition, in which differences in face shape and reflectance were both present.

Last but not least, the comparison between the both-different and the same condition yielded one interesting cluster (cluster 15, Table 2; shown in purple in Fig. 5 coronal view). Located in the right posterior fusiform gyrus (pFus) and extending along the lateral occipitotemporal sulcus (OTS), cluster 15 was the only cluster that showed relatively increased release from adaptation in the both-different condition, compared to the shape-different and reflectance-different conditions (Fig. 6). Note that there was a latency delay in its time course for both reflectance-different and both-different condition. Moreover, its time course data extracted for localizer scans indicate that this

region is object-sensitive, with significantly higher activity to cars than to scrambled cars ($t(13)=3.663$, $P<0.003$) and faces ($t(13)=4.995$, $P<0.0003$). Slightly overlapping with the right FFA and parahippocampal place area (PPA, Epstein and Kanwisher, 1998), its center Talairach coordinates (32, −41, −9) are within the distribution of object-sensitive posterior fusiform/anterior–ventral portion of lateral occipital complex (PF/LOa) reported by Grill-Spector et al. (1999). However, its activation pattern differed somewhat from conventionally defined PF/LOa in that its activation for faces was lower than for scrambled faces and scrambled cars ($t(13)=2.775$, $P<0.02$).

Additional object-sensitive ROI results

The finding of object-sensitive cluster in whole brain analysis led to a further examination of the adaptation release pattern in individually defined object-sensitive areas. Two sub-regions of the lateral occipital complex (LOC, Grill-Spector et al., 1999), namely LO (lateral occipital area) and PF (posterior fusiform area), were localized for each participant using the contrast (cars–scrambled cars). We further excluded the overlap between face-sensitive and object-sensitive regions by eliminating voxels in LOC that showed higher responses for faces than for cars.

Both right (−36±5, −48±9, −15±3, 333 voxels±118, $n=12/14$) and left (−38±5, −47±8, −14±4, 330 voxels±235, $n=8/14$) PF showed significant adaptation release for all three different conditions (all $P<0.05$, Fig. 8). The amount of adaptation release for three different conditions did not differ from each other in either right or left PF (all $P>0.12$). Most importantly, unlike what we observed in the right FFA, the magnitude of adaptation release in the shape-different condition was not larger than that in the reflectance-different condition in the right PF ($t(11)=1.55$, $P>0.15$).

In the right LO (41±5, −70±5, −9±5, 573 voxels±232, $n=14/14$), significant adaptation release was found in shape-different and both-different conditions ($t(13)=4.815$, $P<0.001$ and $t(13)=2.172$, $P<0.05$, respectively), but not in the reflectance-different condition ($t(13)=1.438$, ns). There was also a trend for higher adaptation release in the shape-different condition than in the reflectance-condition in the right LO ($t(13)=2.1$, $P<0.06$). The left LO (−39±5, −71±5, −9±5, 752 voxels±414, $n=12/14$) showed significant adaptation release for shape difference ($t(11)=3.014$, $P<0.02$), a trend for reflectance difference ($t(11)=1.906$, $P<0.08$), but not for their combination ($t(11)=1.31$, $P>0.22$).

Compared to face-sensitive regions, object-sensitive regions showed a somewhat different pattern of adaptation release for changes in face shape and/or reflectance. The most important difference was that the right PF did not show a dominant sensitivity to shape changes over reflectance changes, as found in the right FFA. Also different from whole brain analysis results, individually localized PF did not show an enhanced sensitivity to combined changes in shape and surface reflectance. Note that the average coordinates of individually defined right PF (36, −48, −15) are posterior and lateral to the center coordinates of cluster 15 (32, −41, −9) from the whole brain analysis.

DISCUSSION

In the present study, we used an adaptation paradigm to investigate the representation of shape and surface reflectance information that are diagnostic for individual faces. We focused first on areas that show preferential responses for faces (FFA and OFA). Changes in face shape turned out to be the dominant driving force of the adaptation release in the right FFA and OFA, where stronger release occurred to changes in shape than to changes in surface reflectance. In contrast, surface reflectance was largely represented in areas in the left FFA and OFA, whose releases to changes in reflectance were comparable with those to changes in shape. These results suggest that the representation of shape and surface reflectance in faces is partially overlapping. However, this overlapping organization did not provide a neural counterpart for the behavioral facilitation by the inclusion of both shape and reflectance cues. Indeed, somewhat surprisingly, in all face-sensitive regions, the combined differences in both shape and re-

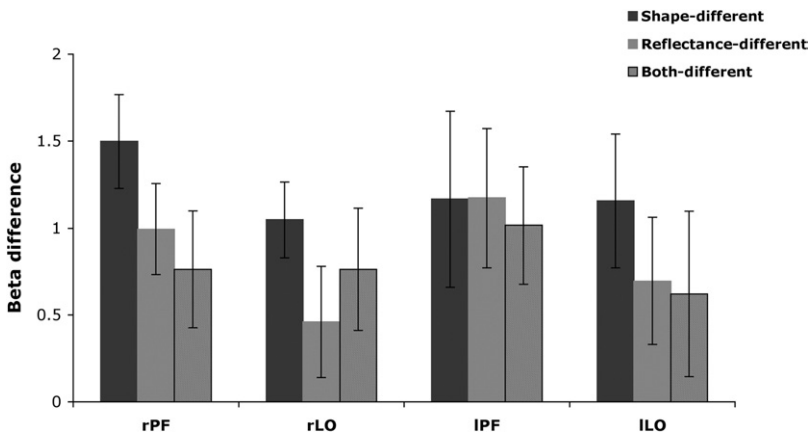

Fig. 8. Illustration of the magnitude of release from adaptation in object-sensitive ROIs in LOC induced by changes in face shape alone (shape-different, black bars), face reflectance alone (reflectance-different, grey bars), or both (both-different, diagonal bars). Beta weights difference was calculated using beta weights in the same condition as baseline.

flectance (both-different condition) did not elicit larger adaptation release than face shape difference did alone.

If face-sensitive areas alone are not good predictors of the behavioral salience of combined face shape and reflectance, where in the brain did the neural integration that accounts for behavioral facilitation take place? Our whole brain analysis revealed an object-selective cluster in the right PF/OTS (adjacent to FFA), whose sensitivity to face shape and reflectance combined was relatively higher than its sensitivity to either property alone. However, a detailed look at individually defined object-sensitive (but not face-sensitive) sub-regions in LOC did not provide further evidence of such neural integration. Given the spatial proximity between face-sensitive and object-sensitive sub-regions in LOC, the integration of shape and surface reflectance cues consistent with the behavioral facilitation may possibly rely on the interaction of multiple high-level visual areas.

Admittedly, the fact that we did not find a stronger release from adaptation in the face-sensitive areas for the both-different condition than for the shape-different condition was an unexpected result. Indeed, participants performed better with faces differing in both shape and reflectance, which were judged as the most different and were also physically the most different. However, the disagreement between the neural response pattern in face-sensitive areas and the physical/perceptual data might help us to further explore the nature of neural representations in face-sensitive areas, if the data are carefully modeled/interpreted (see Andresen et al., 2009). As mentioned previously, a stronger adaptation release to combined changes in two cues than to changes in one cue alone relies on the assumption that the sensitivities to two cues are linearly additive in a coincident brain area. If this assumption were not met in face-sensitive areas, we would not observe the expected increase in release from adaptation. That is, if the sensitivity to individual faces in brain areas such as the right FFA and OFA is driven primarily by global shape, the inclusion of surface reflectance might not provide a substantial additional contribution, or even a (small) negative contribution. In fact, as seen in Fig. 1, the absence of difference in surface reflectance between two subsequently presented faces in the shape-different condition enhances the salience of face shape as a whole, by reducing the local difference (such as the difference in the border of eyebrows, iris, or lips). This could, in turn, facilitate the global process of face shape in this condition, giving rise to the stronger sensitivity to face shape than to the combination of face shape and reflectance found in face-sensitive areas in the right hemisphere.

This interpretation may explain why changes in face shape turned out to be the dominant driving force of the adaptation release in the right FFA and OFA. Besides the right hemisphere's general dominance for 3D perception (Durnford and Kimura, 1971), a right hemispheric superiority has generally been associated with a global or holistic mode of processing faces (Parkin and Williamson, 1987; Sergent, 1989; Hillger and Koenig, 1991), in particular in the right FFA (Schiltz and Rossion, 2006). In contrast, processing local details of faces reduces or abolishes the right hemispheric dominance (Hillger and Koenig, 1991; Rossion et al., 2000). Hence, it may be that the right face-sensitive areas show a maximal release from adaptation for face shape alone because they discriminate faces primarily on the basis of information at a global level (e.g., head shape variations). Paradoxically, adding reflectance to the faces (in the both-different condition) does not increase the release from adaptation, but slightly decreases it, since different reflectance cues come into play for individual face discrimination at a more local level.

If this interpretation is correct, it leads to the prediction that manipulations that affect most global/holistic face processing such as inversion (Yin, 1969; Farah et al., 1995; Rossion, 2008), misalignment of parts (Young et al., 1987) or scrambling of the face features (Tanaka and Farah, 1993) should decrease performance to a greater extent for shape diagnostic faces than for reflectance diagnostic faces. This is precisely what our post-scanning behavioral results indicate. Inversion disrupted shape information more than reflectance information, and, most importantly, than the combination of shape and reflectance information. This happened presumably because in the shape only condition, the global cues conveyed by shape were difficult to process at inverted orientation. However, adding reflectance cues to these faces allowed participants to discriminate the inverted faces better because these cues could be resolved more locally. In other words, holistic processing of faces appears to depend more on shape than reflectance cues, at least with the kind of stimuli used in the present study in which global head shape contours are preserved (unlike in Russell et al., 2007). These observations, made outside of the scanner with an additional group of participants, suggest that the largest release from adaptation found for face shape change alone in the right face-sensitive areas in our neuroimaging study does not necessarily violate the logic of fMR adaptation. Rather, it suggests that the release from adaptation in the right hemisphere face-sensitive areas in particular is largely based on (global) shape cues between individual faces, and that adding diagnostic reflectance information may rather decrease the effect by making shape cues less salient.

Another prediction that could also be tested is that acquired patients who suffer from prosopagnosia following right hemispheric lesions (Sergent and Signoret, 1992; Barton et al., 2002; Bouvier and Engel, 2006) should not only be in trouble when having to process faces as whole configurations (e.g. Sergent and Villemure, 1989; Levine and Calvanio, 1989; Barton et al., 2002), but also present larger impairments at processing faces differing in shape than in reflectance only.

Although changes in face shape and reflectance are well detected in face-sensitive areas, their neural integration consistent with the behavioral facilitation may recruit other non-face sensitive brain areas along the visual pathway. The finding of the cluster in right PF/OTS, which is adjacent to FFA, suggests the possible involvement of object-selective areas in such neural integration. It has been reported previously that right PF/OTS, the anterior-ventral portion of LOC, is sensitive to different viewpoints

and illumination directions of the same face/car (Grill-Spector et al., 1999). The right PF/OTS, therefore, could be a part of generic system that extracts the 3D shape and removes 3D ambiguities. The complementary role of object-selective area in face processing has also been detailed in a recent study by Dricot et al. (2008). Using fMR-adaptation, Dricot and her colleagues found larger responses to different faces than to repeated presentation of the same face in the ventral part of the LOC, both for normal observers and an acquired prosopagnosic patient.

Interestingly, we found a relative delay in the time course data for reflectance-different condition, in areas such as bilateral FFA and right PF/OTS (Figs. 4, 6). In some cases, it was also true for the both-different condition, where the changes in shape were combined with changes in surface reflectance. It is possible that sensitivity to the individual face may emerge from a first wave of low spatial frequency achromatic information, carried by the global shape, with color and the high spatial frequency information accumulating later (Sergent, 1986; Sugase et al., 1999; Goffaux and Rossion, 2006). However, due to the sluggishness of HRF, we cannot draw any firm conclusion based on these fMRI observations. Interestingly, recent data obtained in an adaptation paradigm with event-related potentials (ERPs) support this temporal prevalence of shape over reflectance information (Caharel et al., 2009).

It is also worth noting that the sensitivity to face shape and face reflectance change was present in bilateral dorsolateral prefrontal cortex (IFG and middle frontal gyrus (MFG)), as revealed by whole brain analysis. It has been shown that IFG and MTG are involved mainly in retrieval of semantic information from faces (Leveroni et al., 2000). Moreover, IFG has been considered as part of an extended system for face recognition (Haxby et al., 2000), which is likely to be modulated by the engageness of the task (cf. Fairhall and Ishai, 2007). In line with this view, we suggested that the adaptation release occurred in the prefrontal regions for face reflectance as well as for face shape largely reflected the task difficulty of these two conditions (Duncan and Owen, 2000; Philiastides and Sajda, 2007).

Finally, our experimental design and manipulation introduced several caveats that need to be mentioned. First, as shown in Table 1, each particular face stimulus was presented eight times in an experimental run, four times being an adaptor and four times being a test face. The repeated presentation might cause some fMRI adaptation across trials, thus leading to an overall smaller adaptation release. Second, due to the use of standard localizer, we failed to localize face sensitive areas other than bilateral FFA and OFA consistently across most of our participants. More sensitive localizer (e.g., Fox et al., 2008b) will be needed to investigate the face network on a broader scale.

CONCLUSION

The present study revealed that while both surface reflectance and shape are equally useful for individualizing faces in matching tasks, the neural correlates of shape versus surface reflectance are partially dissociated in face sensitive areas. Face-sensitive areas of the right hemisphere are more sensitive to shape than to surface reflectance cues, while homologous areas of the left hemisphere appear to process both kinds of cues to a similar extent. Combining these two kinds of cues altogether does not lead to a further increase of neural activation in face-sensitive areas, and suggest that more general object sensitive areas may be involved, together with the interaction among multiple visual areas.

Acknowledgments—This research was supported by an ARC grant 07/12-007 (Communauté Française de Belgique–Actions de Recherche Concertées). Fang Jiang is supported by a Human Frontier Science Program postdoctoral award and Bruno Rossion is supported by the Belgian National Fund for Scientific Research (Fonds de la Recherche Scientifique–FNRS). We would like to thank Alice J. O'Toole and Jody Culham for their comments and suggestion on this study. We also thank Jochen Weber for his help on data analysis. We are especially grateful to two anonymous reviewers for helpful feedback.

REFERENCES

Andresen DR, Vinberg J, Grill-Spector K (2009) The representation of object viewpoint in human visual cortex. Neuroimage 45:522–536.

Barton JJ, Press DZ, Keenan JP, O'Connor M (2002) Lesions of the fusiform face area impair perception of facial configuration in prosopagnosia. Neurology 58:71–78.

Blanz V, Vetter T (1999) A morphable model for the synthesis of 3D faces. In: Computer Graphics Proc. SIGGRAPH'99:187–194.

Bouvier SE, Engel SA (2006) Behavioral deficits and cortical damage loci in cerebral achromatoposia. Cereb Cortex 16:183–191.

Bruce V, Young AW (1998) In the eye of the beholder: the science of face perception. Oxford: Oxford University Press.

Caharel S, Jiang F, Blanz V, Rossion B (2009) Recognizing an individual face: 3D shape contributes earlier than 2D surface reflectance information. Neuroimage 47:1809–1818.

Deichmann R, Gottfried JA, Hutton C, Turner R (2003) Optimized EPI for fMRI studies of the orbitofrontal cortex. Neuroimage 19:430–441.

Dricot L, Sorger B, Schiltz C, Goebel R, Rossion B (2008) The roles of "face" and "non-face" areas during individual face perception: evidence by fMRI adaptation in a brain-damaged prosopagnosic patient. Neuroimage 40:318–332.

Duncan J, Owen AM (2000) Common regions of human frontal lobe recruited by diverse cognitive demands. Trends Neurosci 23(10): 475–483.

Durnford M, Kimura D (1971) Right hemisphere specialization for depth perception reflected in visual field differences. Nature 231:394–395.

Epstein R, Kanwisher N (1998) A cortical representation of the local visual environment. Nature 392:598–601.

Fairhall SL, Ishai A (2007) Effective connectivity within the distributed cortical network for face perception. Cereb Cortex 17:2400–2406.

Farah MJ, Tanaka JW, Drain HM (1995) What causes the face inversion effect? J Exp Psychol Hum Percept Perform 21:628–634.

Fox CJ, Iaria G, Barton JJ (2008a) Disconnection in prosopagnosia and face processing. Cortex 44:996–1009.

Fox CJ, Iaria G, Barton JJ (2008b) Defining the face processing network: optimization of the functional localizer in fMRI. Hum Brain Mapp 30(5):1637–1651.

Gauthier I, Tarr MJ, Moylan J, Skudlarski P, Gore JC, Anderson AW (2000) The fusiform "face area" is part of a network that processes faces at the individual level. J Cogn Neurosci 12:495–504.

Gilaie-Dotan S, Malach R (2007) Sub-exemplar shape tuning in human face-related areas. Cereb Cortex 17:325–338.
Goffaux V, Rossion B (2006) Faces are "spatial"—holistic face perception is supported by low spatial frequencies. J Exp Psychol Hum Percept Perform 32:1023–1039.
Grill-Spector K, Kushnir T, Edelman S, Avidan G, Itzchak Y, Malach R (1999) Differential processing of objects under various viewing conditions in the human lateral occipital complex. Neuron 24: 187–203.
Grill-Spector K, Malach R (2001) FMR-adaptation: a tool for studying the functional properties of human cortical neurons. Acta Psychol 107:293–321.
Grill-Spector K, Malach R (2004) The human visual cortex. Annu Rev Neurosci 27:649–677.
Grill-Spector K, Henson R, Martin A (2006) Repetition and the brain: neural models of stimulus-specific effects. Trends Cogn Sci 10:14–23.
Harris A, Aguirre GK (2008) The representation of parts and wholes in face-selective cortex. J Cogn Neurosci 20:863–878.
Haxby JV, Hoffman EA, Gobbini MI (2000) The distributed human neural system for face perception. Trends Cogn Sci 4:223–233.
Hill H, Schyn PG, Akamatsu S (1997) Information and viewpoint dependence in face recognition. Cognition 62:201–222.
Hillger LA, Koenig O (1991) Separable mechanisms in face processing: evidence from hemispheric specialization. J Cogn Neurosci 3:42–58.
Ishai A (2008) Let's face it: it's a cortical network. Neuroimage 40: 415–419.
Jiang F, Blanz V, O'Toole AJ (2006) Probing the visual representation of faces with adaptation: A view from the other side of the mean. Psychol Sci 17:493–500.
Kanwisher N, McDermott J, Chun MM (1997) The fusiform face area: a module in human extrastriate cortex specialized for face perception. J Neurosci 17:4302–4311.
Kourtzi Z, Kanwisher N (2000) Cortical regions involved in perceiving object shape. J Neurosci 20:3310–3318.
Kourtzi Z, Kanwisher N (2001) Representation of perceived object shape by the human lateral occipital complex. Science 293: 1506–1509.
Kourtzi Z, Erb M, Grodd W, Bülthoff HH (2003) Representation of the perceived 3-D object shape in the human lateral occipital complex. Cereb Cortex 13:911–920.
Lee KJ, Perrett DI (1997) Presentation-time measures of the effects of manipulations in color space on discrimination of famous faces. Perception 26:733–752.
Lee KJ, Perrett DI (2000) Manipulation of colour and shape information and its consequence upon recognition and best-likeness judgments. Perception 29:1291–1312.
Leopold DA, O'Toole AJ, Vetter T, Blanz V (2001) Prototype-referenced shape encoding revealed by high-level after effects. Nat Neurosci 4:89–94.
Leveroni CL, Seidenberg M, Mayer AR, Mead LA, Binder JR, Rao SM (2000) Neural systems underlying the recogniton of familiar and newly learned faces. J Neurosci 20:878–886.
Levine DN, Calvanio R (1989) Prosopagnosia: a defect in visual configural processing. Brain Cogn 10:149–170.
O'Toole AJ, Vetter T, Blanz V (1999) Three-dimensional shape and two-dimensional surface reflectance contributions to face recognition: an application of three-dimensional morphing. Vision Res 39:3145–3155.
Parkin AJ, Williamson P (1987) Cerebral lateralization at different stages of facial processing. Cortex 23:99–110.
Philiastides MG, Sajda P (2007) EEG-informed fMRI reveals spatiotemporal characteristics of perceptual decision making. J Neurosci 27:13082–13091.
Puce A, Allison T, Bentin S, Gore JC, McCarthy G (1998) Temporal cortex activation in humans viewing eye and mouth movements. J Neurosci 18:2188–2199.
Rossion B, Dricot L, DeVolder A, Bodart JM, Crommelinck M, de Gelder B, Zoontjes R (2000) Hemispheric asymmetries for whole-based and part-based face processing in the human fusiform gyrus. J Cogn Neurosci 12:793–802.
Rossion B, Caldara R, Seghier M, Schuller AM, Lazeyras F, Mayer E (2003) A network of occipito-temporal face-sensitive areas besides the right middle fusiform gyrus is necessary for normal face processing. Brain 126:2381–2395.
Rossion B (2008) Picture-plane inversion leads to qualitative changes of face perception. Acta Psychol 128:274–289.
Russell R, Sinha P, Biederman I, Nederhouser M (2006) Is pigmentation important for face recognition? Evidence from contrast negation. Perception 35:749–759.
Russell R, Biederman I, Nederhouser M, Sinha P (2007) The utility of surface reflectance for the recognition of upright and inverted faces. Vision Res 47:157–165.
Russell R, Sinha P (2007) Real-world face recognition: the importance of surface reflectance properties. Perception 36:1368–1374.
Sadr J, Sinha P (2004) Object recognition and random image structure evolution. Cogn Sci 28:259–287.
Schiltz C, Rossion B (2006) Faces are represented holistically in the human occipito-temporal cortex. Neuroimage 32:1385–1394.
Sergent J (1986) Microgenesis of face perception. In: Aspects of face processing (Ellis HD, Jeeves MA, Newcombe F, Young AW, eds), pp 17–33. Dordrecht: Martinus-Nijhoff.
Sergent J (1989) Structural processing of faces. In: Handbook of research on face processing (Young AW, Ellis HD, eds), pp 57–91. Amsterdam: North-Holland.
Sergent J, Ohta S, MacDonald B (1992) Functional neuroanatomy of face and object processing: a positron emission tomography study. Brain 115:15–36.
Sergent J, Signoret JL (1992) Implicit access to knowledge derived from unrecognized faces in prosopagnosia. Cereb Cortex 2:389–400.
Sergent J, Villemure JG (1989) Prosopagnosia in a right hemispherectomized patient. Brain 112:975–995.
Sugase Y, Yamane S, Ueno S, Kawano K (1999) Global and fine information coded by single neurons in the temporal visual cortex. Nature 400:869–873.
Talairach G, Tournoux P (1988) Co-planar stereotaxic atlas of the human brain. New York: Thieme.
Tanaka JW, Farah MJ (1993) Parts and wholes in face recognition. Q J Exp Psychol A 46:225–245.
Thomas C, Avidan G, Humphreys K, Jung KJ, Gao F, Behrmann M (2008) Reduced structural connectivity in ventral visual cortex in congenital prosopagnosia. Nat Neurosci 12:29–31.
Tovee MJ (1996) An introduction to the visual system. Cambridge: Cambridge University Press.
Troje NF, Bülthoff HB (1996) Face recognition under varying poses: the role of texture and shape. Vision Res 36:1761–1771.
Vuong QC, Peissig JJ, Harrison MC, Tarr MJ (2005) The role of surface pigmentation for recognition revealed by contrast reversal in faces and Greebles. Vision Res 45:1213–1223.
Winston JS, Henson RN, Fine-Goulden MR, Dolan RJ (2004) fMRI-adaptation reveals dissociable neural representations of identity and expression in face perception. J Neurophysiol 92(3):1830–1839.
Yin RK (1969) Looking at upside-down faces. J Exp Psychol 81: 141–145.
Yip A, Sinha P (2001) Role of color in face recognition. J Vision 2(7):596a.
Young AW, Hellawell D, Hay DC (1987) Configurational information in face perception. Perception 16:749–759.

(Accepted 28 July 2009)
(Available online 4 August 2009)